Crystal structure and physical properties of a novel Kondo antiferromagnet: $U_3Ru_4Al_{12}$

2009 J. Phys.: Condens. Matter 21 125401

(http://iopscience.iop.org/0953-8984/21/12/125401)

IOP PUBLISHING JOURNAL OF PHYSICS: CONDENSED MATTER

J. Phys.: Condens. Matter **21** (2009) 125401 (5pp) doi:10.1088/0953-8984/21/12/125401

Crystal structure and physical properties of a novel Kondo antiferromagnet: $U_3Ru_4Al_{12}$

M Pasturel[1], O Tougait[1,3], M Potel[1], T Roisnel[1], K Wochowski[2], H Noël[1] and R Troć[2]

[1] Sciences Chimiques de Rennes, Université Rennes 1, UMR CNRS 6226, Campus de Beaulieu, 263 avenue Général Leclerc, F-35042 Rennes Cedex, France
[2] Institute of Low Temperature and Structure Research, Polish Academy of Sciences, ulica Okólna 2, 50-422 Wrocław, Poland

E-mail: olivier.tougait@univ-rennes1.fr

Received 17 December 2008, in final form 28 January 2009
Published 26 February 2009
Online at stacks.iop.org/JPhysCM/21/125401

Abstract

A novel ternary compound $U_3Ru_4Al_{12}$ has been identified in the U–Ru–Al ternary diagram. Single-crystal x-ray diffraction indicates a hexagonal $Gd_3Ru_4Al_{12}$-type structure for this uranium-based intermetallic. While this structure type usually induces geometrically a spin-glass behaviour, an antiferromagnetic ordering is observed at $T_N = 8.4$ K in the present case. The reduced effective magnetic moment of U atoms ($\mu_{eff} = 2.6\ \mu_B$) can be explained by Kondo-like interactions and crystal field effects that have been identified by a logarithmic temperature dependence of the electrical resistivity, negative values of the magnetoresistivity and particular shape of the Seebeck coefficient.

(Some figures in this article are in colour only in the electronic version)

1. Introduction

Phase relations and properties in the U–Ru–Al ternary system have not been extensively explored so far. The equiatomic compound URuAl with hexagonal ZrNiAl-type structure has been the only phase reported in the literature. It exhibits a paramagnetic spin fluctuation behaviour at low temperatures [1, 2] without a magnetically ordered state down to 20 mK [1]. At present, the U–Ru–Al isothermal section at 973 K is being experimentally investigated and the existence of new ternary phases has been revealed. The overall results will be published elsewhere. In this paper, $U_3Ru_4Al_{12}$ has been investigated in detail. The crystal structure has been determined by single-crystal x-ray diffraction. The results of measurements of magnetic susceptibility, electrical resistivity, magnetoresistivity and thermoelectric power on polycrystalline samples of $U_3Ru_4Al_{12}$ are presented and discussed in this paper.

[3] Author to whom any correspondence should be addressed.

2. Experimental details

The samples have been prepared by arc-melting of the elemental components (all purities above 99.9%), turned and remelted several times to ensure homogeneity. Then, the samples were placed in alumina crucibles, enclosed under vacuum in sealed silica tubes and annealed for at least two weeks at 973 K. The purity of the phases was checked by x-ray powder diffraction (Cu Kα_1 radiation, $\lambda = 1.5406$ Å) and SEM–EDS analysis.

Single-crystal x-ray diffraction was performed on a four-circle Nonius Kappa CCD diffractometer (Mo Kα, $\lambda = 0.710\,73$ Å) at room temperature. Reflections collected on half the Ewald sphere were integrated using the Denzo–Scalepack software [3]. The structure was solved by direct methods using SIR97 [4] and refined using SHELXL-97 [5] available in the WinGX package [6] after semi-empirical absorption corrections [7].

Magnetic properties were investigated in the temperature range 2–300 K and magnetic fields up to 5 T, using a superconducting quantum interference device (SQUID) magnetometer.

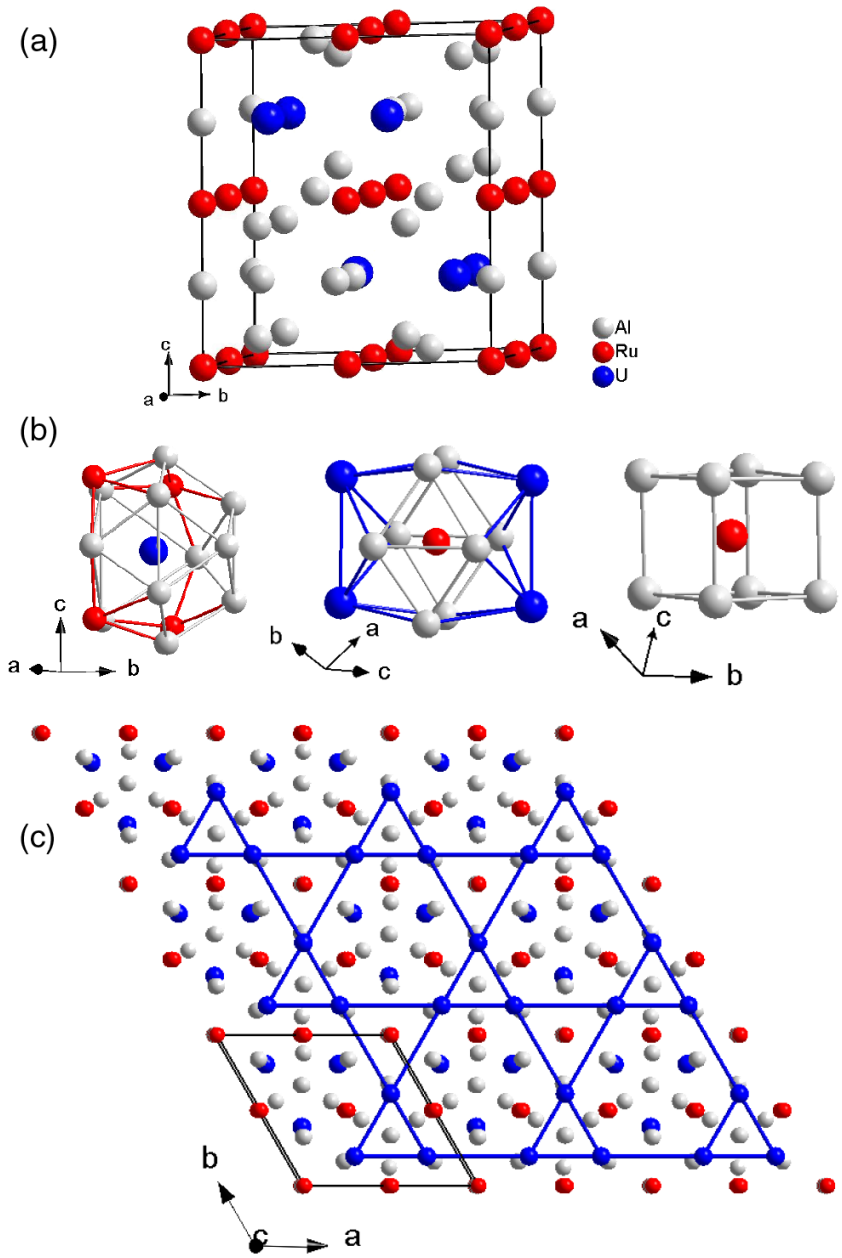

Figure 1. (a) Crystal structure of $U_3Ru_4Al_{12}$, (b) coordination spheres of U, Ru1 and Ru2 atoms in this structure and (c) projection of the structure in the (a, b) plane highlighting the Kagomé lattice.

Electrical resistivity and magnetoresistivity measurements were performed down to liquid helium temperature in applied magnetic fields up to 8 T. The Seebeck coefficient was measured in the temperature range 5–300 K by the steady-state method.

3. Results and discussion

3.1. Crystal structure

Crystallographic measurements have been performed on a $U_3Ru_4Al_{12}$ small single crystal extracted from a bulk sample with the same nominal composition. The data collection conditions and refinement results are presented in table 1. Collected reflections are indexed in a primitive hexagonal unit cell with the cell parameters $a = 8.8300(1)$ Å and $c = 9.4296(2)$ Å. Observed extinctions and refinement results indicate the $P6_3/mmc$ space-group (no. 194) and refined atomic positions (table 2) are consistent with the $Gd_3Ru_4Al_{12}$ structure type [8] for this novel intermetallic (figure 1). This structure type has already been encountered for other uranium aluminides, such as $U_3Co_{4+x}Al_{12-x}$ [9] and $U_3Fe_4Al_{12}$ [10]. The coordination sphere of uranium atoms is composed by 4 Ru atoms and 11 Al atoms (figure 1(b) and table 3). The Ru1 and Ru2 atoms are, respectively, surrounded by a strongly distorted [U_4Al_8] icosahedron and [Al_8] cube (figure 1(b) and table 3). In this structure, the uranium atoms are located in a plane perpendicular to the c axis, forming a distorted

Table 1. Crystallographic data and structure refinement for $U_3Ru_4Al_{12}$.

Empirical formula	$U_3Ru_4Al_{12}$
Formula weight (g mol^{-1})	1442.13
Structure type	$Gd_3Ru_4Al_{12}$
Space group	$P6_3/mmc$ (no 194)
Unit cell parameters (Å)	$a = 8.8300(1)$
	$c = 9.4296(2)$
Unit cell volume (Å^3)	636.71(2)
Z/calculated density (g cm^{-3})	2/7.522
Absorption coefficient (mm^{-1})	43.413
Crystal size (mm × mm × mm)	0.20 × 0.08 × 0.06
Theta range	2.66°–45.27°
Limiting indices	$-17 \leqslant h \leqslant 13$
	$-14 \leqslant k \leqslant 17$
	$-16 \leqslant l \leqslant 18$
Collected/unique reflections	25 697/1045
R (int)	0.1435
Absorption correction	Semi-empirical
Max./min. transmission	0.1245/0.0148
Data/restraints/parameters	1045/0/27
Goodness of fit on F^2	1.172
R indices [$I > 2\sigma(I)$]	$R1 = 0.037$
	$wR2 = 0.086$
Extinction coefficient	0.0051(5)
Largest difference peak and hole (e Å^{-3})	+5.708/−3.198

Table 2. Refined atomic parameters and equivalent isotropic displacement parameters (Å^2) for $U_3Ru_4Al_{12}$.

	Wyckoff position	x	y	z	Ueq (Å^2)
U	6h	0.1951(1)	0.3902(1)	1/4	0.015(1)
Ru1	6g	1/2	0	0	0.014(1)
Ru2	2a	0	0	0	0.014(1)
Al1	12k	0.1619(1)	0.3238(2)	0.5777(2)	0.016(1)
Al2	6h	0.5610(1)	0.1219(3)	1/4	0.015(1)
Al3	4f	1/3	2/3	0.0189(3)	0.016(1)
Al4	2b	0	0	1/4	0.016(1)

Kagomé lattice (figure 1(c)) [9] with small triangles (d_{U-U} = 3.662(1) Å) being connected to three large triangles (d_{U-U} = 5.168(2) Å). In this structure type, the shortest U–U distances are above Hill's criterion favouring magnetic ordering but the Kagomé triangular geometry usually favours magnetic frustration, and the two previously cited compounds with the same stoichiometry exhibit just spin-glass behaviour [9–11].

3.2. Magnetic properties

The temperature dependence of the magnetic susceptibility of $U_3Ru_4Al_{12}$ and its inverse are presented in figure 2. The temperature variation of the susceptibility (upper inset in figure 2) shows the occurrence of an antiferromagnetic transition at T_N = 8.4 K, confirmed by ac susceptibility measurements (not shown here). The paramagnetic domain is well fitted using a modified Curie–Weiss law (full line in figure 2) between 30 and 400 K, giving a temperature-independent term $\chi_0 = 0.47 \times 10^{-3}$ emu mol^{-1}, a paramagnetic Curie temperature $\theta_p = -21$ K and a

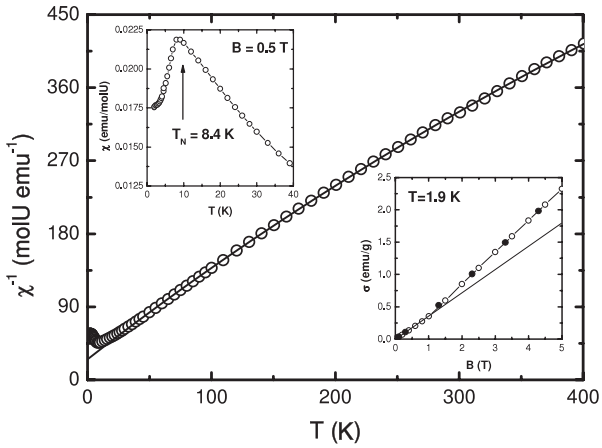

Figure 2. Temperature dependence of the inverse magnetic susceptibility of $U_3Ru_4Al_{12}$ (open symbols). The solid line corresponds to a modified Curie–Weiss fit of the paramagnetic domain. The inset on the left shows the low temperature dependence of the susceptibility. The inset on the right presents the field dependence of the magnetization at T = 1.9 K.

Table 3. Selected interatomic distances (Å) in $U_3Ru_4Al_{12}$.

U-1 Al4	2.984(1)	Ru1-2 Al2	2.535(1)
-2 Al3	3.036(2)	-2 Al3	2.555(1)
-2 Al2	3.038(2)	-4 Al1	2.688(1)
-2 Al1	3.131(2)	-4U	3.337(1)
-4 Al1	3.207(1)		
-4 Ru1	3.337(1)	Ru2-2 Al4	2.357(1)
		-6 Al1	2.582(2)
U-2U	3.662(1)		
-2U	5.168(2)		

reduced effective magnetic moment per uranium atom μ_{eff} = 2.6 μ_B/U. This hints towards an influence of the crystal field interaction of the ligands surrounding the central uranium ion in this aluminide (figure 1(b)). The field dependence of the magnetization (lower inset in figure 2) is reversible, with only a slight deviation from initial linearity above 1 T, towards another linear domain with larger slope (i.e. susceptibility). This deviation is not clear at present without performing further magnetization measurements in higher magnetic fields.

3.3. Transport properties

The resistivity and magnetoresistivity measurement results are presented in figure 3. From 140 K down to T_N, the resistivity of $U_3Ru_4Al_{12}$ increases slightly with decreasing temperature, following the equation: $\rho(T) = (\rho_0 + \rho_0^\infty) + c_K \ln T$ (solid line in figure 3(a)) appropriate for scattering of conduction electrons on imperfections, disordered spins and Kondo impurities, respectively. A least-squares fit of this equation to the experimental data yields the following parameters: $(\rho_0+\rho_0^\infty) = 419\ \mu\Omega$ cm and $c_K = -13.9\ \mu\Omega$ cm. This $\ln T$ variation of electrical resistivity is typical for compounds exhibiting Kondo interactions [12, 13], which can also be responsible for the reduced effective moment of uranium atoms. A distinct maximum in $\rho(T)$ is observed close to T_N and then the resistivity decreases with further

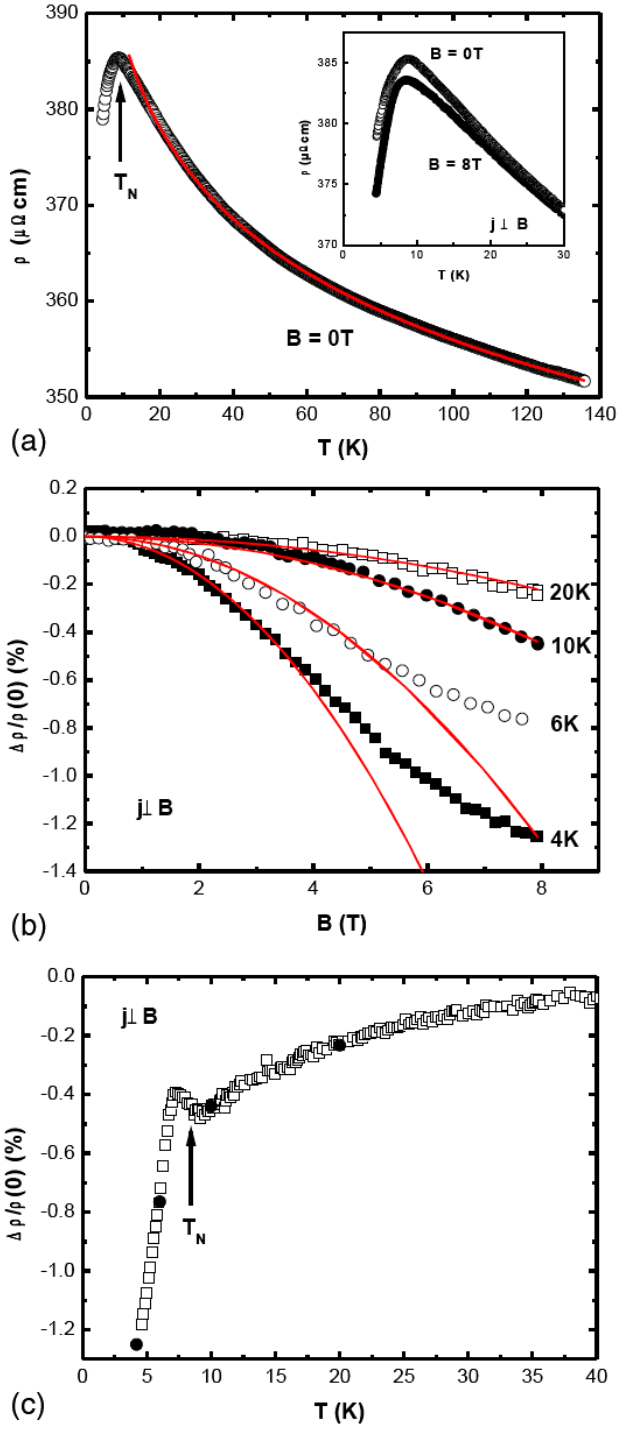

Figure 3. (a) Temperature dependence of the electrical resistivity of $U_3Ru_4Al_{12}$ without applied magnetic field. The solid line corresponds to a $\ln T$ fit of the experimental data. The inset shows the difference at low temperature with the resistivity measured under an applied magnetic field of 8 T perpendicular to the current; (b) magnetic field dependence of the magnetoresistivity at four different temperatures. Solid lines correspond to the $-\alpha B^2$ fit of the experimental data; (c) temperature dependence of the magnetoresistivity under an applied magnetic field of 8 T. The four black dots correspond to the values obtained in (b) at $B = 8$ T.

lowering temperature. This maximum is probably caused by the antiferromagnetic order having a magnetic unit cell different from the crystallographic one.

Field and temperature dependences of the transverse magnetoresistivity (TMR) ($\mu_0 H \perp i$), defined as $\Delta\rho/\rho_0 = (\rho(B) - \rho(0))/\rho(0)$, were measured and the results are presented in figures 3(a)–(c). The values of the resistivity at low temperature are slightly decreased under a magnetic field of 8 T applied perpendicular to the current (inset in figure 3(a)). The field dependence of TMR taken at different temperatures (figure 3(b)) shows that (i) only a moderate and negative magnetoresistive effect occurs and (ii) the character of the TMR curve is different in the paramagnetic and magnetically ordered state. Above T_N, the $\Delta\rho/\rho_0 = f(B)$ curves follow a $-\alpha B^2$ law (solid lines in figure 3(b)), as is usually observed in Kondo systems [14–17]. At temperatures lower than T_N, a deviation from this law is observed at high magnetic fields where the S-shaped curves appear. A similar behaviour is explained by metamagnetic transitions in the Kondo antiferromagnet $U_2Co_6Al_{19}$ [18]. The temperature dependence of $\Delta\rho/\rho_0$ under an applied magnetic field of 8 T (figure 3(c)) confirms these observations: $\Delta\rho/\rho_0$ slowly decreases with temperature from 40 to 9 K, turns up around the antiferromagnetic transition (between 9 and 7 K), then goes through a small peak and finally decreases sharply with temperature in the magnetically ordered state. Although the TMR magnitudes are rather small, the increasing negative magnitude of TMR in the antiferromagnetic region below T_N is difficult to explain. This behaviour can be compared with that of another antiferromagnet UNiAl which revealed a similar peak close to T_N in $\Delta\rho/\rho_0(T)$ [19], but in contrast to $U_3Ru_4Al_{12}$ its TMR decreased in absolute value below T_N, reaching very small values close to $T = 0$ K. Nevertheless, we think that, as for UNiAl, the occurrence of the peak in $\Delta\rho/\rho_0(T)$ just below T_N for $U_3Ru_4Al_{12}$ is due to the change in the Brillouin zone due to the forming of a complex magnetic structure in the antiferromagnetic region.

The Seebeck coefficient of $U_3Ru_4Al_{12}$ (figure 4) is negative at high temperature and presents a broad minimum at about 225 K where it reaches a minimum value of -13 μV K^{-1}. Below this temperature it decreases in absolute value with decreasing temperature to turn positive at 12(1) K and then presents also a positive peak at $T_{max} = 8(1)$ K where the compound orders antiferromagnetically. These variations are expected for a Kondo compound in the presence of crystal electrical field effects [20, 21], in agreement with magnetic, electrical resistivity and magnetoresistivity properties. Almost identical behaviour has been previously observed for UCu_5In [22] which crystallizes in an orthorhombic structure and being also an antiferromagnet with $T_N = 25$ K. The change in sign observed for these two compounds at temperatures close to their T_N can be attributed to a change in the density of states near the Fermi level due to a reconstruction of the Fermi surface. The sign change of thermopower (TEP) in the semi-phenomenological model [23] can be ascribed to the development of magnetic correlations at low temperature. The strong correlations in $U_3Ru_4Al_{12}$ are also highlighted on the $T/S = f(T^2)$ plot (inset of figure 4), where two linear domains are observed at high temperature, following the Hirst two-band model (from [24]), especially adapted to the

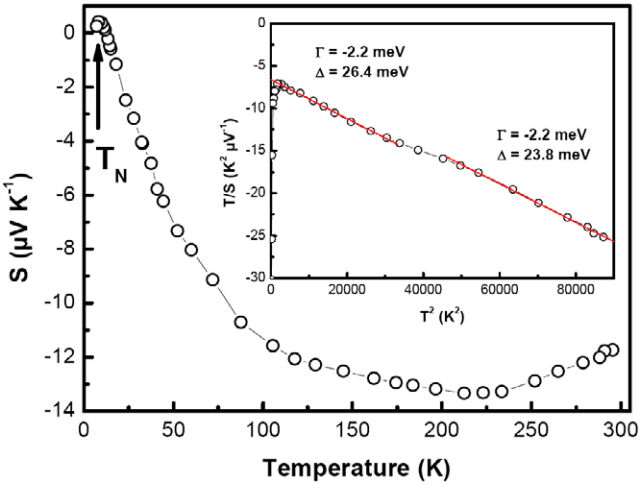

Figure 4. Temperature dependence of Seebeck coefficient of $U_3Ru_4Al_{12}$. The inset presents the linear behaviour of $T/S = f(T^2)$; solid lines correspond to a fit using the Hirst model.

case of the intermediate valence compounds:

$$S(T) = \frac{AT}{B^2 + T^2} \qquad \text{with} \qquad A = \frac{2\Delta}{|e|}$$

$$\text{and} \qquad B^2 = \frac{3(\Delta^2 + \Gamma^2)}{(\pi k_B)^2} \tag{1}$$

where $\Delta = \varepsilon_{5f}$–$\varepsilon_F$ is a measure of the position of the 5f density of states peak with respect to the Fermi level and Γ is the width of the Lorentzian-shaped 5f band. The fitting of the two domains using the previous equations gives the same $\Gamma = -2.2$ meV in both cases and $\Delta = 26.4$ meV at $T < 200$ K and 23.8 meV at $T > 200$ K. The existence of two linear domains and the values of Γ and Δ are comparable with the results obtained by Park *et al* [25] on the moderate heavy fermions $CeAl_2$ and UAl_2. The low temperature variation of TEP of UNiAl is also due to the appearance of magnetic zone boundaries resulting from the antiferromagnetic order with a similar effect as was observed in the temperature variation of the resistivity of this aluminide [26].

4. Conclusion

The novel $U_3Ru_4Al_{12}$ intermetallic compound crystallizes in the hexagonal $Gd_3Ru_4Al_{12}$ structure type. Despite the distorted Kagomé lattice formed by uranium atoms, an antiferromagnetic ordering occurs at $T_N = 8.4$ K. The reduced effective moment carried by U atoms can possibly be understood by invoking Kondo and crystal field effects that influence the electrical resistivity, the magnetoresistivity and the Seebeck coefficient. Neutron diffraction experiments are planned to be performed in order to solve the magnetic structure.

Acknowledgments

The authors are grateful to Mrs S Casale and I Péron for SEM–EDS analyses, as well as Dr C Sułkowski, Mr R Gorzelniak and D Badurski for assistance in physical measurements.

This work is financially supported by the Polish Academy of Sciences (PAN)—French National Center for Scientific Research (CNRS) exchange project no. 14473.

References

[1] Sechovsky V, Havela L, De Boer F R, Franse J J M, Veenhuizen P A, Sebek J, Stehno J and Andreev A V 1986 *Physica* B+C **142** 283
[2] Samsel-Czekala M, Talik E and Troć R 2008 *Phys. Rev.* B **78** 245120
[3] Otwinowski Z and Minor W 1997 Processing of x-ray diffraction data collected in oscillation mode, methods in enzymology *Macromolecular Crystallography, part A* vol 276, ed C W Carter Jr and R M Sweet (New York: Academic) pp 307–26
[4] Altomare A, Burla M C, Camalli M, Cascarano G L, Giacovazzo C, Guagliardi A, Moliterni A G G, Polidori G and Spagna R 1999 *J. Appl. Crystallogr.* **32** 115
[5] Sheldrick G M 1998 Programs for Crystal Structure Analysis (Release 97-2) Institüt für Anorganische Chemie der Universität, Tammanstrasse 4, D-3400 Göttingen, Germany
[6] Farrugia L J 1999 *J. Appl. Crystallogr.* **32** 837
[7] Blessing R H 1995 *Acta Crystallogr.* A **51** 33
[8] Tougait O, Noel H and Troć R 2004 *J. Solid State Chem.* **177** 2053
[9] Gonçalves A P, Waerenborgh J C, Gaczynski P, Noël H and Tougait O 2009 *Intermetallics* **17** 25
[10] Tougait O, Noel H and Troć R 2007 *Phil. Mag.* **87** 1085
[11] Cornut B and Coqblin B 1972 *Phys. Rev.* B **5** 4541
[12] Edelstein A S 2003 *J. Magn. Magn. Mater.* **256** 430
[13] Chevalier B, Garcia Soldevilla J, Gomez Sal J C, Barandiaran J M and Etourneau J 1999 *J. Magn. Magn. Mater.* **196/197** 878
[14] Yamauchi R and Fukamichi K 2000 *J. Phys.: Condens. Matter* **12** 2461
[15] Ragel F C, du Plessis P de V and Strydom A M 2007 *J. Phys.: Condens. Matter* **19** 506211
[16] Tchoula Tchokonté M B, du Plessis P de V, Kaczorowski D and Strydom A M 2008 *Physica* B **403** 1350
[17] Troć R, Noël H, Tougait O and Wochowski K 2004 *J. Phys.: Condens. Matter* **16** 3097
[18] Schoenes J, Troisi F, Brück E and Menovsky A A 1992 *J. Magn. Magn. Mater.* **108** 40
[19] Troć R 2006 *J. Alloys Compounds* **423** 21
[20] Bhattacharjee A K and Coqblin B 1976 *Phys. Rev.* B **13** 3441
[21] Zlatić V, Horvatić B, Milat I, Coqblin B, Czycholl G and Grenzebach C 2003 *Phys. Rev.* B **68** 104432
[22] Kaczorowski D, Troć R, Czopnik A, Jeżowski A, Henkie Z and Zaremba V I 2001 *Phys. Rev.* B **63** 144401
[23] Fischer K H 1989 *Z. Phys.* B **76** 315
[24] Gottwick U, Gloos K, Horn S, Steglich F and Grewe N 1985 *J. Magn. Magn. Mater.* **47/48** 536
[25] Park J-G and Očko M 1997 *J. Phys.: Condens. Matter* **9** 4627
[26] Prokeš K, Fukuda S and Sakurai J 1999 *Physica* B **270** 221